

Structure of phospholipid-cholesterol membranes: An x-ray diffraction study

Sanat Karmakar* and V. A. Raghunathan†
Raman Research Institute, Bangalore 560080, India
 (Received 16 December 2004; published 29 June 2005)

We have studied the phase behavior of mixtures of cholesterol with dipalmitoyl phosphatidylcholine (DPPC), dimyristoyl phosphatidylcholine (DMPC), and dilauroyl phosphatidylethanolamine (DLPE), using x-ray diffraction techniques. Phosphatidylcholine (PC)-cholesterol mixtures are found to exhibit a modulated phase for cholesterol concentrations around 15 mol % at temperatures below the chain melting transition. Lowering the relative humidity from 98% to 75% increases the temperature range over which it exists. An electron density map of this phase in DPPC-cholesterol mixtures, calculated from the x-ray diffraction data, shows bilayers with a periodic height modulation, as in the ripple phase observed in many PCs in between the main- and pretransitions. However, these two phases differ in many aspects, such as the dependence of the modulation wavelength on the cholesterol content and thermodynamic stability at reduced humidities. This modulated phase is found to be absent in DLPE-cholesterol mixtures. At higher cholesterol contents the gel phase does not occur in any of these three systems, and the fluid lamellar phase is observed down to the lowest temperature studied (5 °C).

DOI: 10.1103/PhysRevE.71.061924

PACS number(s): 87.16.Dg, 61.30.-v, 61.10.Eq

I. INTRODUCTION

Phospholipids and cholesterol are important constituents of plasma membranes [1]. There is some evidence for the existence of cholesterol rich lipid domains, called rafts, in these membranes, which are suspected to play a vital role in many cellular events [2–5]. Although a wide variety of phospholipids are present in cell membranes, the major ones are phosphatidylcholines (PC) and phosphatidylethanolamines (PE). Therefore, PC-cholesterol and PE-cholesterol mixtures are excellent model systems to study the effect of cholesterol on lipid membranes. There have been many studies on the thermotropic phase behavior of phospholipid-cholesterol mixtures using a variety of experimental techniques [6–14]. Some of these studies surmise the coexistence of a cholesterol-rich (l_o) and a cholesterol-poor (l_d) phase in these bilayers above the chain melting transition of the lipid ($T > T_m$), at cholesterol concentrations (X_c) in the range 10–20 mol % [11,15,16]. But other experimental techniques, such as x-ray diffraction and fluorescence microscopy, do not show any evidence of phase separation of two fluid phases in these binary systems [17]. On the other hand, x-ray diffraction studies on dimyristoyl phosphatidylcholine (DMPC)-cholesterol mixtures have indicated phase separation at high temperatures (>50 °C) for $10 < X_c < 20$, which is believed to arise from two different arrangements of cholesterol molecules in the bilayer [18]. Studies on phospholipid-cholesterol monolayers have also suggested the formation of complexes at specific stoichiometric ratios [19].

Dipalmitoyl phosphatidylcholine (DPPC) and DMPC exhibit the ripple ($P_{\beta'}$) phase, characterized by a periodic height modulation of the bilayers, between the L_{α} and L_{β} phases at high hydration. This phase is absent in PEs, and the

L_{α} phase transforms directly into L_{β} on cooling. This difference in phase behavior is believed to arise from the existence of a nonzero chain-tilt in the gel phase of PCs. Incorporation of cholesterol into a PC bilayer modifies the ripple wavelength (λ). It is found from earlier freeze fracture studies on DMPC-cholesterol bilayers that λ increases with X_c from ~ 200 Å at 0 mol % to ~ 500 Å at 20 mol % [20]. The ripple phase is not observed for $X_c > 20$ mol %. A similar trend has been observed in neutron scattering studies on DMPC-cholesterol mixtures [21]. In these studies, λ is also found to be strongly temperature dependent. We have recently reported a different kind of modulated phase (denoted as P_{β}) in DPPC-cholesterol mixtures at $12.5 \leq X_c \leq 22$ [22,23]. This phase is distinct from the ripple ($P_{\beta'}$) phase seen in these systems in between the main- and pretransition temperatures.

In this paper we present results of x-ray diffraction studies on oriented multilayers of binary mixtures of cholesterol with DPPC, DMPC, and dilauroyl phosphatidylethanolamine (DLPE). These lipids were chosen in order to study the influence of the chain length and the nature of the head group on the phase behavior of lipid-cholesterol mixtures. Partial phase diagrams of these systems have been constructed from the diffraction data at 98% and 75% relative humidity (RH). The phase behavior of DMPC-cholesterol bilayers is found to be very similar to that of DPPC-cholesterol mixtures. On the other hand, the behavior of the DLPE-cholesterol system is different in that it does not exhibit the modulated (P_{β}) phase. We believe that this difference in the phase behavior is related to the fact that the hydrocarbon chains are not tilted with respect to the bilayer normal in the gel phase of DLPE.

II. MATERIALS AND METHODS

DPPC and DMPC were purchased from Fluka, whereas DLPE and cholesterol were obtained from Sigma. They were used without further purification. For x-ray diffraction experiments, appropriate amounts of the lipid and cholesterol

*Electronic address: sanat@rri.res.in

†Electronic address: varaghu@rri.res.in

were dissolved in chloroform. Typical total (lipid + cholesterol) concentration was ~ 5 mg/ml. Fifteen DPPC-cholesterol mixtures were prepared with X_c ranging from 0 to 55 mol %. Eight DLPE-cholesterol and six DMPC-cholesterol mixtures, with X_c ranging from 0 to $\sim 30\%$, were also studied. The solution was deposited on a cylindrical glass substrate with a radius of curvature of ~ 15 mm. The area density of the lipid film was $\sim 5 \mu\text{g mm}^{-2}$. The sample was kept for ~ 12 h inside an evacuated desiccator to remove traces of the solvent. It was then hydrated for a couple of days in a water-saturated atmosphere. This results in well-aligned multilayers of the phospholipid-cholesterol mixture. These hydrated samples were transferred to a sealed chamber with mylar windows for the experiments. The x-ray beam from a rotating anode generator (Rigaku UltraX18) operating at 50 kV and 80 mA was tangential to the cylindrical substrate, with the cylinder axis normal to the beam. The wavelength, selected using a flat graphite monochromator, was 1.54 \AA . A beam size of ~ 1 mm was obtained at the sample using two pairs of slits. Sample temperature was controlled to an accuracy of ± 0.1 °C using a circulating water bath. Diffraction patterns were recorded on a 2D image plate detector of 180 mm diameter and 0.1 mm pixel size (Marresearch). The sample to detector distance was in the range 200–250 mm. All samples were first heated to a temperature much above the main transition temperature of the lipid and then cooled to 5 °C in steps of 5 °C. The diffraction patterns were recorded mainly during cooling from the L_α phase, but we also monitored the phase behavior during the initial heating of some of the samples. Relative humidity (RH) was kept fixed at $98 \pm 2\%$, by keeping a reservoir of water in the sealed chamber. Data were also collected from some samples at a lower RH of 75%, which was achieved by using a saturated aqueous solution of sodium chloride instead of water. The sample temperature and the RH close to the sample were measured with a thermo-hygrometer (Testo 610) inserted into the chamber. Typical exposure time was ~ 1 h.

III. EXPERIMENTAL RESULTS

Small angle scattering techniques can in principle detect microscopic phase separation in the plane of bilayers, if there is sufficient contrast in the scattering densities of the two phases. However, even in the absence of such contrast, macroscopic phase separation can easily be detected from non-overlapping reflections in the diffraction pattern coming from the individual phases. On the basis of the diffraction patterns we have determined partial phase diagrams of the three binary systems. Since we use oriented samples, the in-plane ordering of molecules can be easily inferred from the wide angle reflections. For example, in the gel phase of DPPC, we see two wide angle reflections, one on-axis ($q_z = 0$) and the other off-axis ($q_z \neq 0$), coming from the quasi-hexagonal lattice of hydrocarbon chains of the lipid molecules. The wide angle spot at $q_z \neq 0$ indicates that the molecules are tilted with respect to the bilayer normal and that the direction of the tilt is toward nearest neighbor [24].

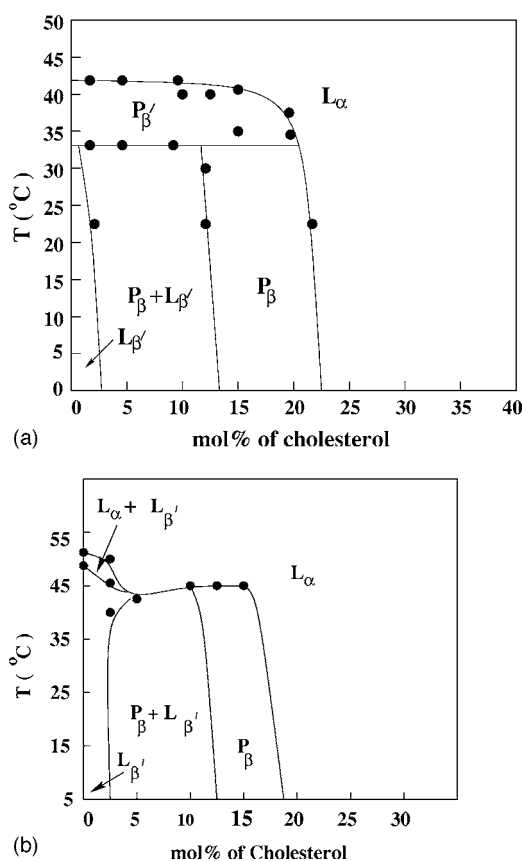


FIG. 1. The phase diagrams of DPPC-cholesterol mixtures at 98% RH (a) and 75% RH (b), determined from the diffraction data.

A. DPPC-cholesterol

Phase diagrams of this system at 98% and 75% RH have been constructed from the diffraction data and are presented in Fig. 1. The gel ($L_{\beta'}$) phase was identified from the presence of sharp chain reflections in the wide angle region of the diffraction pattern [25], whereas the modulated (P_β) phase was identified from the presence of “satellite” reflections in the small angle region [Figs. 2 and 3(a)]. The latter phase is characterized by a rectangular unit cell, unlike the usual ripple ($P_{\beta'}$) phase, occurring in between the pre- and main-transitions, which has an oblique unit cell [Fig. 3(b)]. The transition temperatures of DPPC are in agreement with earlier reports [26]. Two distinct wide angle reflections, one on-axis and the other off-axis, in the gel phase clearly show that the chains are tilted with respect to the layer normal, toward one of their nearest neighbors. Tilt angle can be measured from the positions of these two reflections and is found to be $\sim 30^\circ$. Incorporation of 2.5 to 10 mol % cholesterol does not affect the main- and pretransitions significantly. The diffraction pattern of the ripple phase suggests an increase in the wavelength with cholesterol content, as found in earlier studies [7,20]. For $2.5 < X_c < 12.5$, below pretransition we observe two sets of reflections in the small angle region, indicating the coexistence of the gel and P_β phases [Fig. 4(a)]. The coexistence of these two phases persists even at low temperatures down to 5 °C. At $X_c = 12.5$ mol % the P_β phase appears at ~ 31 °C and continues down to 25 °C. Below 25 °C it coexists with $L_{\beta'}$.

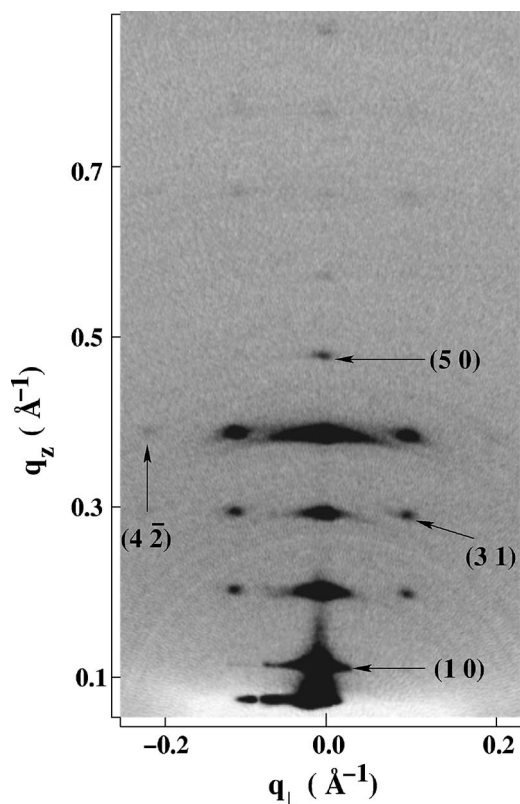


FIG. 2. The diffraction pattern of the P_β phase of DPPC-cholesterol mixtures at RH=98% ($X_c=15$ mol %, $T=6$ °C). The reflections can be indexed on a primitive rectangular lattice as shown. The q scales are approximate and are intended only as guides.

For $15 < X_c < 20$, pretransition disappears and the P_β phase exists down to the lowest temperature studied (5 °C). Increasing X_c further leads to a fluid phase, often called the liquid ordered (l_o) phase in the literature [Fig. 4(b)]. As can be seen from this figure the wide angle chain reflections get condensed along q_z in the presence of cholesterol, due to the stretching of the chains. In addition, the spacing of these reflections also changes with X_c . For example, it changes from 4.2 to 4.9 Å as X_c is increased from 20 to 55 mol % at 25 °C. The phase boundary between l_o and P_β is detected at $X_c=22$ mol %. For $X_c \geq 50$ mol % we obtain diffraction patterns with a large number of sharp reflections on initial heating of the sample. This structure melts into the l_o phase at ~ 50 °C on heating and is not seen on cooling down to 5 °C. This structure was not probed in any detail in the present study. The diffraction data at 98% RH are summarized in Table I.

At 75% RH the $P_{\beta'}$ phase is found to be absent, in agreement with earlier studies [25]. On the other hand, the P_β phase is stabilized at this lower humidity and occurs over a wide range of temperature from 45 °C to 5 °C [Fig. 1(b)]. The range of X_c over which it is found is very similar to that at 98% RH, although the $P_{\beta'}-l_o$ boundary is shifted to a slightly lower value of X_c .

The modulation wavelength λ of the P_β phase is found to vary both with temperature and X_c , as shown in Fig. 5. At 5 °C, $\lambda \sim 65$ Å both at 98% and 75% RH. Although it in-

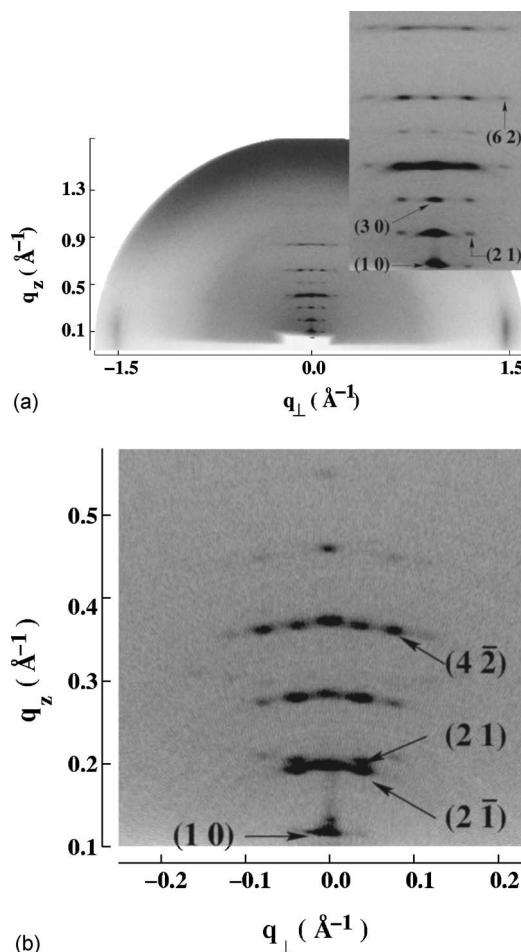


FIG. 3. (a) The diffraction pattern of the P_β phase of DPPC-cholesterol mixtures at 75% RH ($X_c=12.5$ mol %, $T=21$ °C, $d=61.4$ Å, $\lambda=67.5$ Å). The inset shows the small angle region of the diffraction pattern on an expanded scale. The reflections can be indexed on a primitive rectangular lattice as shown. For comparison the diffraction pattern of the ripple ($P_{\beta'}$) phase of DMPC ($T=20$ °C, RH=98%), which occurs in between the pre- and main transitions, is shown in (b) ($d=57.6$ Å, $\lambda=158.4$ Å). These reflections can be indexed on an oblique lattice as shown. The q scales are approximate and are intended only as guides.

creases significantly with temperature, it never reaches values comparable to the modulation wavelength of the $P_{\beta'}$ phase, which is typically in the range 150–200 Å. λ decreases with X_c , with the rate of decrease increasing considerably on approaching the $P_{\beta'}-l_o$ phase boundary.

B. DMPC-cholesterol

The phase behavior of DMPC-cholesterol mixtures was found to be very similar to that of DPPC-cholesterol mixtures (Fig. 6). Distinct satellites from the P_β phase were not observed at 98% RH even at 5 °C, but this phase could easily be identified from the smearing of the lamellar peaks along q_\perp . Good diffraction patterns of this phase were obtained in DPPC-cholesterol mixtures only at temperatures well below the pretransition. The fact that the pretransition temperature of DMPC is much lower (~ 13 °C) than that of

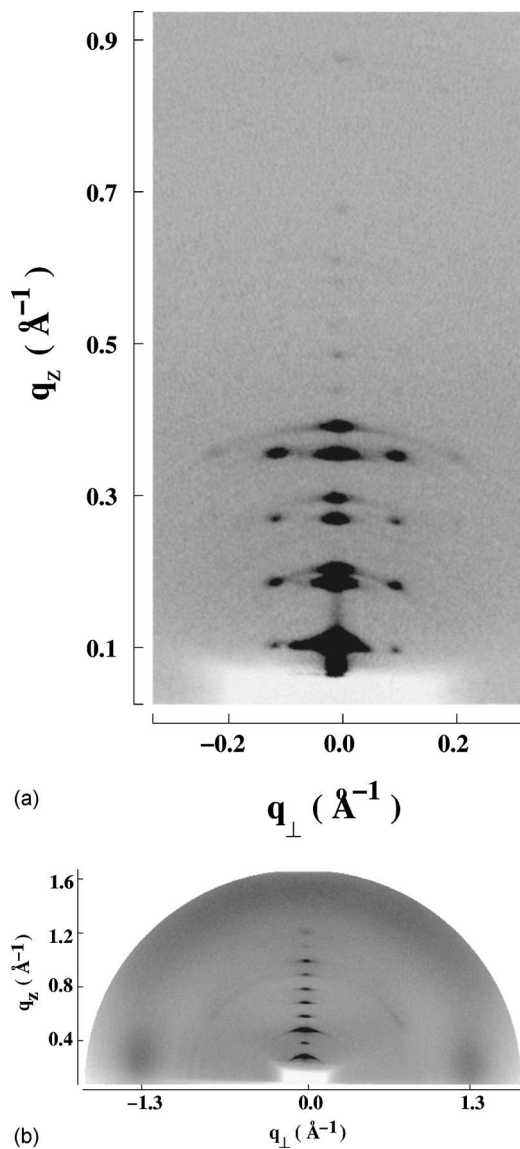


FIG. 4. (a) The diffraction pattern showing the coexistence of the gel and P_β phases ($X_c=10$ mol %, $T=10$ °C, RH=98%). (b) The diffraction pattern of the cholesterol-rich l_o phase ($X_c=50$ mol %, $T=55$ °C, RH=98%). In (b) the first-order lamellar peak is masked by the beam stop. The q scales are approximate and are intended only as guides.

DPPC (~ 33 °C) might explain the difficulty in obtaining good diffraction patterns of this phase in DMPC-cholesterol mixtures. The coexistence of P_β and gel phases is observed at intermediate cholesterol concentrations as in DPPC-cholesterol mixtures. Distinct satellites from P_β phase are observed in the diffraction pattern at 75% RH, when the chain melting transition of the lipid occurs at a much higher temperature [25]. Further, as in DPPC-cholesterol mixtures, this phase is stable over a much larger temperature range at the lower humidity.

C. DLPE-cholesterol

The main transition of DLPE occurs at around 30 °C. A typical diffraction pattern of the gel phase is shown in Fig. 7.

The wide angle reflection at $q_z=0$ indicates that there is no tilt of the hydrocarbon chains with respect to the bilayer normal. Incorporation of cholesterol into DLPE bilayers facilitates the formation of a highly ordered phase (Fig. 8), which transforms at around 45 °C into the L_α phase. On cooling, the L_α phase continues down to 30 °C, at which temperature the L_β is formed. We do not observe the highly ordered phase on cooling, even at the lowest temperature studied (5 °C). However, it is formed on incubating the sample at this temperature for a few hours; the presence of cholesterol seems to make this transformation much faster, as reported earlier by McMullen *et al.* [27].

In the 5 mol % cholesterol mixture we observe two sets of lamellar reflections; one of them has spacing comparable to that of the gel phase, and the other one is similar to cholesterol-rich l_o phase. This observation is in agreement with the previous report by Takahashi *et al.* [28]. For $X_c \geq 10$ mol %, we observe only the l_o phase throughout the temperature range studied. The spacings of the different phases in DLPE-cholesterol mixtures are given in Table II, and the partial phase diagram deduced from the diffraction data is shown in Fig. 9.

IV. ELECTRON DENSITY MAP OF THE P_β PHASE

It is clear from the diffraction patterns that the P_β phase has a simple rectangular unit cell. The bilayers in this phase, therefore, must have a periodic modulation. We take this to be a height modulation, as in the ripple ($P_{\beta'}$) phase. We rule out a thickness modulation of the bilayers, since packing considerations in such a case can be expected to favor a centered rectangular unit cell.

The electron density can be calculated from the diffraction data, once the phases of the different reflections are known. Since the structure is taken to be centrosymmetric, the phases are either 0 or π , and were determined using a modeling procedure used earlier for the $P_{\beta'}$ phase [29,30]. The electron density within the unit cell $\rho(r)$ can be described as the convolution of a contour function $C(x,z)$ and a transbilayer profile $T(x,z)$, i.e., $\rho(r)=C(x,z)\otimes T(x,z)$. $C(x,z)=\delta[z-u(x)]$, where $u(x)$ describes the bilayer height profile. The calculated structure factors F_c are the Fourier transform $F(\vec{q})$ of $\rho(r)$ sampled at the reciprocal lattice points. From the convolution theorem it follows that $F(\vec{q})$ is given by

$$F(\vec{q}) = F_C(\vec{q})F_T(\vec{q}) \quad (1)$$

where $F_C(\vec{q})$ and $F_T(\vec{q})$ are the Fourier transforms of $C(x,z)$ and $T(x,z)$, respectively.

$u(x)$ is assumed to have a triangular shape, given by

$$\begin{aligned} u(x) &= \frac{2A}{\lambda} \left(x + \frac{\lambda}{2} \right) & -\frac{\lambda}{2} \leq x < -\frac{\lambda}{4} \\ &= -\frac{2A}{\lambda} x & -\frac{\lambda}{4} \leq x \leq \frac{\lambda}{4} \\ &= \frac{2A}{\lambda} \left(x - \frac{\lambda}{2} \right) & \frac{\lambda}{4} < x \leq \frac{\lambda}{2}, \end{aligned}$$

TABLE I. The lamellar spacings d (Å) of DPPC-cholesterol mixtures as a function of temperature. Two sets of spacings indicate the coexistence of the $L_{\beta'}$ and P_{β} phases. Numbers in brackets correspond to the wavelength (λ) of the P_{β} or the $P_{\beta'}$ phase. * and † denote the ripple ($P_{\beta'}$) and P_{β} phases, respectively, which were identified from the smearing of the lamellar reflections. RH=98±2%. The error in d is ±0.3 Å.

T (°C)	X_c (mol %)									
	0	5	10	15	20	22	33	40	45	50
45	56.6	...	59.1	59.2	59.2	60.6	60.7	61.0	59.7	59.1
40	62.3 (145)	61.5*	62.9*	63.5	62.6	63.1	60.7	61.0	59.7	59.5
35	60.3*	61.0*	62.9*	65.4†	63.9†	63.8	60.7	61.0	59.7	57.8
30	60.0	59.2, 61.5†	61.4, 66.0(84.9)	65.7(79.5)	63.9(74.0)	63.8	60.7	61.0	59.4	58.4
25	59.7	59.5, 64.0(75.8)	62.0, 67.4(77.7)	65.7(66.8)	63.9(63.2)	63.8	60.7	62.1	60.5	58.8
20	63.9	59.5, 64.0(70.6)	60.8, 66.8(75.5)	67.0(66.8)	67.4(60.7)	65.3	60.7	62.1	60.8	59.5
15	62.0	59.7, 64.6(68.9)	60.3, 66.8(69.3)	66.7(63.0)	67.4(60.7)	65.3	60.7	61.9	60.4	58.3
10	62.0	59.7, 64.6(68.9)	60.3, 66.5(67.9)	66.7(63.0)	67.4(58.3)	65.3(51.2)	60.7	61.3	60.2	58.4
5	60.3, 66.5(66.6)	66.3(60.7)	...	65.3(51.2)	...	61.6	59.9	58.2

where A and λ are the amplitude and the wavelength of the modulation, respectively.

$T(x, z)$ consists of three δ functions, two with positive amplitude (ρ_H) corresponding to the head group regions at the surfaces of the bilayer and one with negative amplitude (ρ_M) corresponding to the methyl group region at the center of the bilayer. It is given by

$$T(x, z) = \delta(x)[\rho_H[\delta(z + z_o) + \delta(z - z_o)] - \rho_M\delta(z)]. \quad (2)$$

z_o is the position of the head group with respect to the center of the bilayer.

Fourier transforming this expression, we get

$$F_T(\vec{q}) = \rho_M \left(\frac{2\rho_H}{\rho_M} \cos(z_o q_z) - 1 \right). \quad (3)$$

We also used a model, where the three δ functions were replaced with Gaussians. In the Gaussian model, $F_T(\vec{q})$ can be written as

$$F_T(\vec{q}) = \sigma_m \rho_M \left(\frac{2\rho_H \sigma_h}{\sigma_m \rho_M} [e^{-q^2 \sigma_h^2 / 2} \cos(q z_o)] - e^{-q^2 \sigma_m^2 / 2} \right), \quad (4)$$

where σ_h and σ_m are the widths of the Gaussians corresponding to head group and terminal methyl group regions, respectively. We have also considered a model with five δ functions, the two additional ones of amplitude ρ_C taking into account the secondary maxima in the electron density due to cholesterol [17].

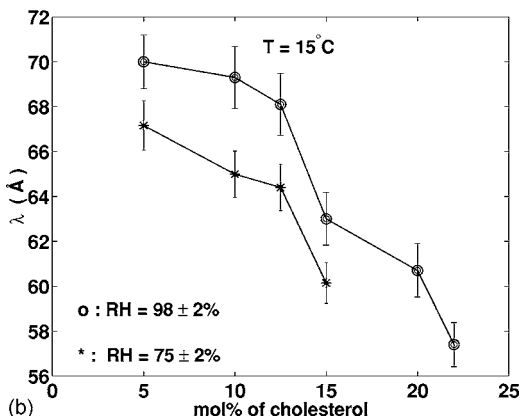
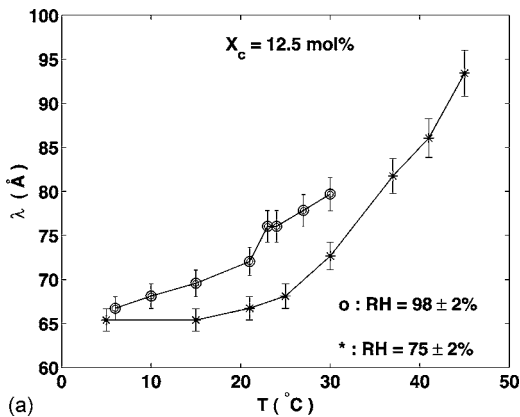


FIG. 5. The variation of the modulation wavelength (λ) of the P_{β} phase of DPPC-cholesterol mixtures with temperature at $X_c = 12.5$ mol % (a) and with X_c at $T = 15$ °C (b).

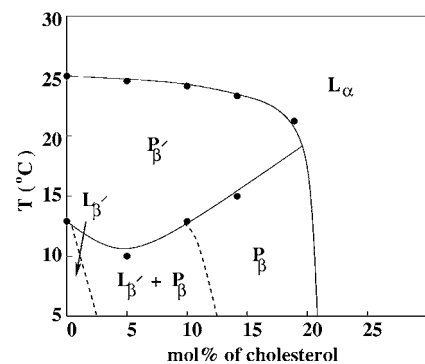


FIG. 6. The phase diagram of DMPC-cholesterol mixtures at 98% RH, determined from the diffraction data. The phase boundaries indicated by dotted lines have not been determined very precisely.

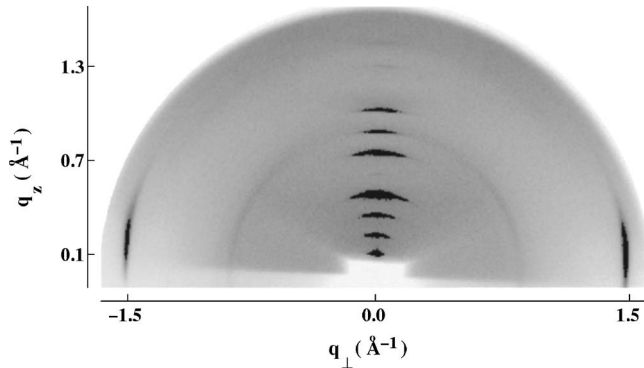


FIG. 7. The diffraction pattern of the L_β phase of DLPE ($T=10$ °C, RH=98%). The absence of chain tilt is indicated by the on-axis ($q_z=0$) wide-angle reflections. The shadow at the bottom is due to the absorption by the substrate. The q scales are approximate and are intended only as guides.

The observed structure factor magnitudes ($|F_o^{hk}|$) were obtained from the integrated intensity calculated from the diffraction data ($|F_o^{hk}|=\sqrt{I^{hk}}$). Geometric corrections to the observed intensities, relevant to the present experimental geometry, are discussed in Ref. [30]. We have not applied absorption corrections to the observed intensities as it is difficult to measure the thickness of the sample precisely. We have found from earlier studies on the $P_{\beta'}$ phase that these corrections do not affect the electron density maps significantly [30]. We would expect a similar situation in the present case, too.

Parameters in these models, such as ρ_H , ρ_M , ρ_C , and the bilayer thickness, were determined by fitting the calculated structure factors with the observed ones. This was done by using the standard Levenberg Marquardt technique for non-linear least squares fitting [31]. Phases obtained from the three δ function and five δ function models are the same for all strong reflections, but phases of a few weak reflections do change with the starting values of the material parameters. But a model with five Gaussians could not be used, since the model parameters did not converge, probably due to the large number of parameters in it. Structure factors obtained from the fit and from the diffraction data are given in Table III.

TABLE II. The lamellar spacings d (Å) of DLPE-cholesterol mixtures as a function of temperature. RH=98±2%. Two sets of spacings indicate the coexistence of L_α and L_β phases. The error in d is ± 0.3 Å.

T (°C)	X_c (mol %)							
	0	2.5	5	7.5	10	15	20	30
45	43.6	43.1	43.2	43.3	44.0	45.5	45.8	46.2
40	43.6	44.1	43.5	43.4	44.7	46.6	46.1	46.7
35	44.1	44.6	44.1	44.5	45.2	47.1	46.4	46.8
30	48.1	45.2; 47.7	45.3; 47.5	45.6	45.8	47.4	47.1	46.8
25	48.4	47.8	47.8; 48.1	47.4; 48.7	47.6	48.1	48.1	46.8
20	48.9	48.6	48.2	48.4	47.9	49.1	48.3	47.8
15	49.3	48.6	48.4	48.4	48.3	49.1	48.4	47.8
10	49.5	48.6	48.4	48.4	47.9	49.3	48.4	47.8

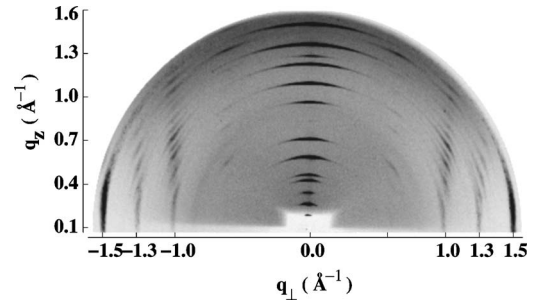


FIG. 8. The diffraction pattern of a highly ordered phase of DLPE-cholesterol mixtures observed in samples before heating to high temperatures ($X_c=10$ mol %). The q scales are approximate and are intended only as guides.

Converged values of the model parameters are given in Table IV. The calculated phases (Φ^{hk}) were combined with the observed magnitudes and inverse Fourier transformed to get the two-dimensional electron density map, shown in Fig. 10, using the expression,

$$\rho(x, z) = \sum_{h,k} F_o^{hk} e^{i\Phi^{hk}} \cos(q_x^{hk}x + q_z^{hk}z). \quad (5)$$

We have also constructed a one-dimensional electron density profile of the l_o phase using the three and the five δ function models, as well as the three Gaussian model. Phases obtained from all the models are the same, except for those of a few weak reflections, but, as would be expected, the Gaussian model gives a better fit to the experimental data, compared to the other two. The trans-bilayer electron density profiles of DPPC and DLPE mixtures in the l_o phase, obtained using the three Gaussian model, are presented in Figs. 11(a) and 11(b). The observed and calculated structure factors are given in Table V. The electron density profiles calculated using the phases obtained from the other two models are very similar to those shown in Figs. 11(a) and 11(b). Therefore, the phases of some of the weak reflections, which depend on the model used, are uncertain.

V. DISCUSSIONS

The results presented above show that the modulated (P_β) phase differs in many ways from the ripple ($P_{\beta'}$) phase. First

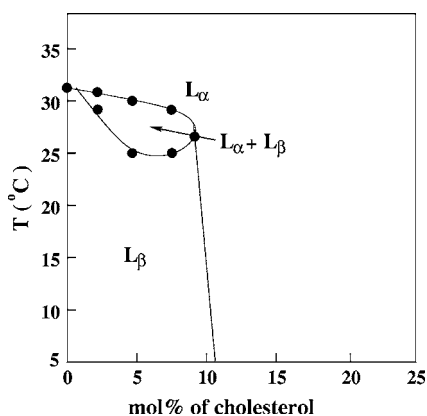


FIG. 9. The phase diagram of DLPE-cholesterol mixtures at 98% RH, determined from the diffraction data.

of all, $P_{\beta'}$ is well known to occur only at very high RH, close to 100%. In contrast, P_{β} occurs even at 75% RH. Secondly, the variation of the modulation wavelength (λ) with cholesterol content shows opposite trends in the two phases. In the $P_{\beta'}$ phase λ increases with X_c and seems to diverge near $X_c \sim 20$ mol % [20]. On the other hand, in the P_{β} phase it decreases with X_c and tends to zero at a similar concentration (Fig. 5). These differences confirm our earlier claim [22] that these two phases are distinct. However, we have not been able to determine the distribution of cholesterol in the P_{β} phase bilayers. The electron density map (Fig. 10) suggests that these bilayers have a rather small height modulation, with an amplitude of ~ 2 Å, which is about five times smaller than that seen typically in the $P_{\beta'}$ phase. This map also suggests that the cholesterol concentration within the bilayer alternates periodically between the two monolayers making up a bilayer. Such a distribution of cholesterol would make the bilayer locally asymmetric and can in principle lead to a local curvature of the bilayer. This can explain the observed small amplitude periodic height modulation of the bilayer. However, as we have diffraction data over a very

TABLE III. The observed structure factor magnitudes ($|F_o^{hk}|$) of the P_{β} phase of DPPC-cholesterol mixtures ($X_c=15$ mol %, $T=6$ °C, $\text{RH}=98\pm 2\%$) and their best fit values (F_c^{hk}) obtained from the electron density model.

h	k	$ F_o $	F_c	h	k	$ F_o $	F_c
1	0	10.0	-10.0	2	2	...	-0.49
2	0	7.44	-7.67	2	-2	...	-0.54
3	0	3.86	2.73	3	1	3.25	-1.47
4	0	10.38	-9.99	3	-1	3.25	1.46
5	0	1.27	-2.31	3	2	...	0.44
6	0	0.52	1.30	3	-2	...	0.46
7	0	0.53	-1.79	4	1	6.43	7.99
8	0	0.77	-0.004	4	-1	6.43	-7.89
9	0	1.03	-0.03	4	2	1.09	-3.35
2	1	2.79	2.59	4	-2	1.09	-3.45
2	-1	2.79	-2.57	5	2	...	-1.54
...	5	-2	...	-1.53

TABLE IV. The values of the model parameters obtained from the best fit for a DPPC-cholesterol mixture in the P_{β} phase using the five δ -function model, and for a DPPC-cholesterol and a DLPE-cholesterol mixture in the l_o phase using the three Gaussian model. A is the amplitude of the height modulation in the P_{β} phase. z_o and z_c are the distances of the peaks corresponding to the head group and cholesterol from the center of the bilayer, respectively. σ_h and σ_m are the widths of the Gaussians corresponding to the head group and the terminal methyl group in the three Gaussian model.

Sample	A	z_o	z_c	$\frac{2\rho_H}{\rho_M}$		$\frac{2\rho_C}{\rho_M}$	
				ρ_M	ρ_M	σ_h	σ_m
DPPC-Ch (15%)	8.3	23.3	9.4	2.16	0.38
DPPC-Ch (50%)	...	19.89	...	1.58	...	1.93	5.97
DLPE-Ch (30%)	...	18.0	...	1.57	...	2.28	4.90

limited q -range, we cannot presently rule out the possibility that this short length scale modulation in the cholesterol concentration is an artifact of the Fourier reconstruction of the electron density.

If the basic structural feature of the P_{β} phase is an in-plane modulation in the cholesterol concentration, instead of a height modulation as assumed in the electron density model, one would expect the $(0, k)$ reflections to be very prominent, since they correspond to variations in the electron density, projected onto the plane of the bilayer. We have carried out experiments to check this possibility, by aligning the bilayers normal to the x-ray beam. Although we were able to observe a diffuse wide angle peak from the chains, no peaks were seen in the small angle region corresponding to the $(0, k)$ reflections. This result rules out a structure similar to that of a stripe phase with strong in-plane modulation of cholesterol concentration. On the other hand, this observation is consistent with the structure inferred from the electron

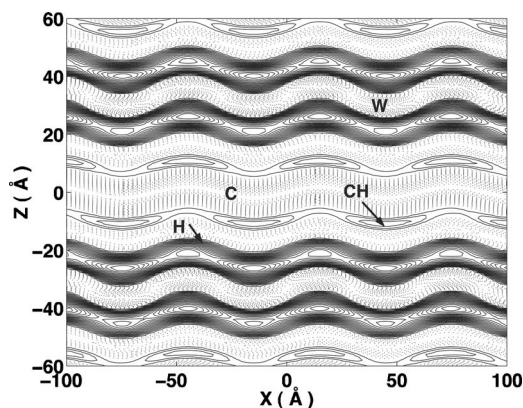


FIG. 10. The electron density map of the P_{β} phase of DPPC-cholesterol mixtures calculated from the diffraction data given in Table III, using the phases obtained with the five δ -function model. The solid (dotted) contours correspond to the electron rich (poor) regions of the bilayer. H, W, and C denote the head group, water, and chain regions of the bilayer. CH denotes the electron-rich band in the bilayer due to the presence of cholesterol. $X_c=15$ mol %, $T=6$ °C, $\text{RH}=98\%$, $d=66.3$ Å, and $\lambda=60.7$ Å.

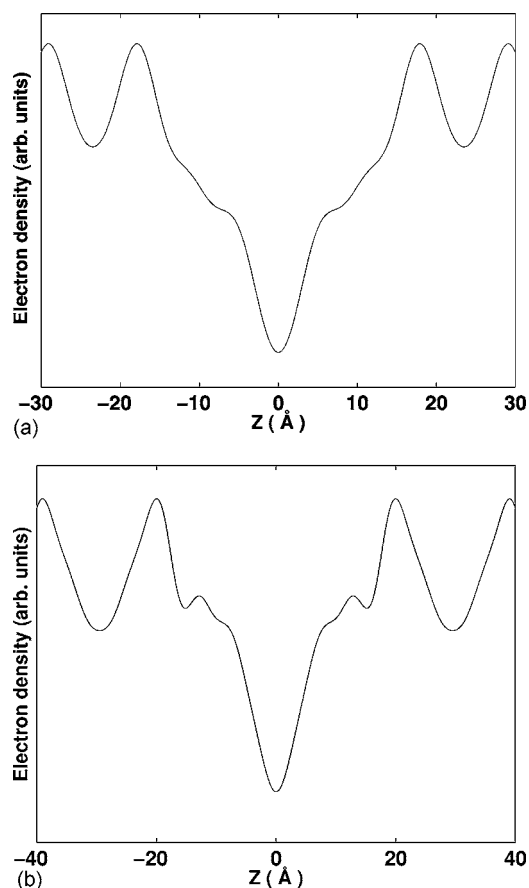


FIG. 11. The transbilayer electron density profile in the l_o phase of (a) DLPE at 30 mol % cholesterol ($T=6$ °C, $RH=98\%$) and (b) DPPC at 50 mol % cholesterol ($T=24$ °C, $RH=98\%$), calculated from the data given in Table V. Peaks near ± 20 Å and the trough at the center correspond to the head groups and terminal methyl groups of hydrocarbon chains, respectively. Peaks near ± 10 Å are due to the presence of cholesterol.

density map, since the intensity of the (0,1) reflection calculated from the model for the values of the parameter obtained from the fit is a few orders of magnitude smaller than that of the (1,0) reflection.

The P_β phase in DPPC-cholesterol mixtures has not been identified in earlier studies. The very small amplitude of the bilayer height modulations must be the reason for its not being seen in freeze fracture electron microscopy studies [20]. However, the coexistence of two lamellar phases has been reported in this system over a range of cholesterol concentration, similar to that over which the gel- P_β coexistence is seen in the present study [32]. It was also reported that the phase coexisting with the gel phase had a higher lamellar spacing, as seen in the present study. In Ref. [32] it was suggested that this increase in d might be the consequence of a decrease in the attractive van der Waals interaction between the bilayers on incorporating cholesterol. However, the fact that the l_o phase with much higher X_c has a smaller d does not support this conjecture. Therefore, it is likely that this increase in d arises from an increase in the steric repulsion between the bilayers resulting from thermal undulations of the bilayers [33]. Indeed some recent studies have indicated a

TABLE V. The observed structure factors ($|F_o^{hk}|$) and their best fit values (F_c^{hk}) obtained from the three Gaussian model for two binary mixtures of cholesterol with DPPC ($X_c=50$ mol %, $RH=98\%$, $T=24$ °C, $d=59.0$ Å) and DLPE ($X_c=30$ mol %, $RH=98\%$, $T=6$ °C, $d=47.0$ Å) in the l_o phase.

h	DPPC-Ch (50%)		DLPE-Ch (30%)	
	$ F_o $	F_c	$ F_o $	F_c
1	10.00	-10.00	10.00	-10.00
2	7.72	-6.96	2.99	-2.71
3	0.78	1.20	0.42	1.06
4	5.16	-2.81	3.68	-2.82
5	0.71	-1.31	0.45	1.45
6	0.82	2.03	0.83	-0.32
7	1.14	-1.03	0.49	-0.23
8	0.54	-0.38	0.39	0.26
9	0.95	0.79
10	...	-0.38
11	0.55	-0.09

softening of the bilayers at comparable cholesterol concentrations [14], which can account for the enhanced thermal undulations. Our preliminary optical microscopy studies on giant unilamellar vesicles made up of these mixtures also show significant thermal shape fluctuations at small values of X_c , revealing an unexpected softening of the bilayers. More quantitative measurements are necessary to confirm this possibility.

The phase behavior of DMPC-cholesterol mixtures is very similar to that of DPPC-cholesterol mixtures. This is not surprising since the phase behaviors of the two lipids themselves are very similar. On the other hand, it is interesting that DLPE-cholesterol mixtures do not exhibit the P_β phase. This difference is most probably related to the fact that the chains are not tilted in the gel phase of DLPE. It is a rather well-established fact that the $P_{\beta'}$ phase occurs only in lipids that exhibit a nonzero chain tilt in the gel phase. Our results indicate that the formation of the P_β phase too is confined to similar lipids. However, studies on other lipid-cholesterol mixtures are necessary to confirm this possibility.

As mentioned in the Introduction, many spectroscopy studies have indicated the coexistence of two fluid phases in binary lipid-cholesterol mixtures at temperatures above the chain melting transition of the lipid. These two phases have been referred to as the liquid ordered (l_o) and the liquid disordered (l_d) phases and occur over a composition range corresponding to $\sim 10 < X_c < \sim 20$ mol %. However, such a phase separation has not been observed in any of the diffraction studies on these mixtures reported in the literature. We also do not see any indication of phase separation in this temperature and composition range. This difference might arise from the fact that spectroscopy techniques are sensitive to local environment of the molecules, whereas the scattering experiments probe the structure at a much longer length scale. It is possible that randomly dispersed microscopic domains with different chain conformation are present in the

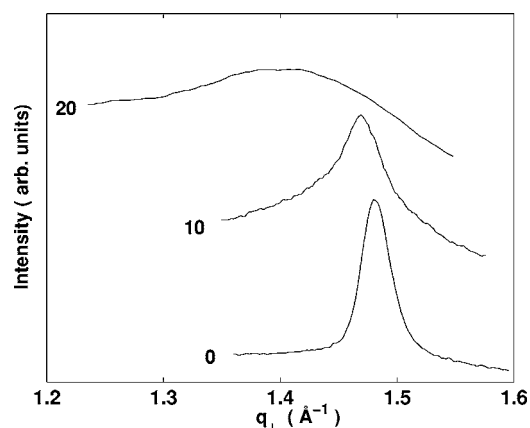


FIG. 12. The wide angle chain reflections of DLPE bilayers at different cholesterol concentrations indicated by the labels on the curves ($T=20\text{ }^{\circ}\text{C}$, $\text{RH}=98\%$).

bilayers, without leading to a macroscopic phase separation.

The condensed wide angle reflection in the l_o phase shows that the hydrocarbon chains of the lipid molecules are stretched by the intercalated cholesterol molecules. The presence of a larger number of lamellar reflections in this phase can be understood in terms of the higher rigidity of the bilayers in the presence of cholesterol [34]. The intensity profiles of the wide angle chain reflections of DLPE at $T=20\text{ }^{\circ}\text{C}$ for a few cholesterol concentrations are plotted in Fig. 12. The wide angle peak is initially sharp in the gel phase, but gets gradually broader as the cholesterol content is

increased, indicating that the correlation length of chain ordering decreases gradually with X_c at temperatures below the chain melting transition. A similar trend has been found in the case of DPPC-cholesterol mixtures [22]. It is interesting to note that the L_{β} phase of DLPE can accommodate about 10 mol % of cholesterol, whereas the $L_{\beta'}$ phase of DPPC and DMPC can incorporate only about 2 mol % of cholesterol. This difference might be related to the fact that the PC-cholesterol mixtures exhibit the P_{β} phase, which has no chain tilt as in the L_{β} phase of DLPE.

VI. CONCLUSION

We have systematically studied the phase behavior of binary mixtures of cholesterol with DPPC, DMPC, and DLPE. A modulated phase is found in PC-cholesterol mixtures at intermediate cholesterol concentrations, whose structure is somewhat similar to that of the ripple phase seen in some PCs in between the main- and pretransitions. These two phases, however, differ in the dependence of their structural parameters on cholesterol concentration and relative humidity. This phase is absent in DLPE-cholesterol mixtures. At higher cholesterol concentrations all the three systems exhibit a fluid lamellar phase, with a higher degree of chain ordering compared to the L_{α} phase of the pure lipids.

ACKNOWLEDGMENTS

We thank Madan Rao, Satyajit Mayor, Yashodhan Hatwalne, and Peter Laggner for many useful discussions and M. Mani for technical assistance.

-
- [1] See, for example, L. Finegold, ed., *Cholesterol in Membrane Models* (CRC Press, Boca Raton, FL, 1993).
- [2] D. A. Brown and E. London, *J. Biol. Chem.* **275**, 17221 (2000).
- [3] C. Dietrich, L. A. Bagatolli, Z. N. Volovyk, N. L. Thompson, M. Levi, K. Jacobson, and E. Gratton, *Biophys. J.* **80**, 1417 (2001).
- [4] J. R. Silvius, *Biochim. Biophys. Acta* **1610**, 174 (2003).
- [5] M. Edidin, *Annu. Rev. Biophys. Biomol. Struct.* **32**, 257 (2003).
- [6] P. F. F. Almeida, W. L. C. Vaz, and T. E. Thompson, *Biochemistry* **31**, 6739 (1992).
- [7] W. Knoll, G. Schmidt, K. Ibel, and E. Sackmann, *Biochemistry* **24**, 5240 (1985).
- [8] M. R. Vist and J. H. Davis, *Biochemistry* **29**, 451 (1990).
- [9] T. P. W. McMullen, R. N. A. H. Lewis, and R. N. McElhaney, *Biochemistry* **32**, 516 (1993).
- [10] S. W. Hui and N. B. He, *Biochemistry* **22**, 1159 (1983).
- [11] M. B. Sankaram and T. E. Thompson, *Proc. Natl. Acad. Sci. U.S.A.* **88**, 8686 (1991).
- [12] B. R. Lentz, D. A. Barrow, and M. Hoehli, *Biochemistry* **19**, 1943 (1980).
- [13] C. Paré and M. Lafleur, *Biophys. J.* **74**, 899 (1998).
- [14] M. Rappolt, M. F. Vidal, M. Kriechbaum, M. Steinhart, H. Amenitsch, S. Bernstorff, and P. Laggner, *Eur. Biophys. J.* **31**, 575 (2003).
- [15] J. H. Ipsen, G. Karlström, O. G. Mouritsen, H. Wennerström, and M. J. Zuckermann, *Biochim. Biophys. Acta* **905**, 162 (1987).
- [16] A. Filippov, G. Orädd, and G. Lindblom, *Biophys. J.* **84**, 3079 (2003).
- [17] T. J. McIntosh, *Biochim. Biophys. Acta* **513**, 43 (1978).
- [18] F. Richter, G. Rapp, and L. Finegold, *Phys. Rev. E* **63**, 051914 (2001).
- [19] A. Radhakrishnan, T. G. Anderson, and H. M. McConnell, *Proc. Natl. Acad. Sci. U.S.A.* **97**, 12422 (2000).
- [20] B. R. Copeland and H. M. McConnell, *Biochim. Biophys. Acta* **599**, 95 (1980).
- [21] K. Mortensen, W. Pfeiffer, E. Sackmann, and W. Knoll, *Biochim. Biophys. Acta* **945**, 221 (1988).
- [22] S. Karmakar and V. A. Raghunathan, *Phys. Rev. Lett.* **91**, 098102 (2003).
- [23] S. Karmakar, V. A. Raghunathan, and S. Mayor, *J. Phys.: Condens. Matter* **17**, S1177 (2005).
- [24] M. Hentschel and R. Hosemann, *Mol. Cryst. Liq. Cryst.* **94**, 291 (1983).
- [25] G. S. Smith, E. B. Sirota, C. R. Safinya, R. J. Plano, and N. A. Clark, *J. Chem. Phys.* **92**, 4519 (1990).
- [26] M. J. Janiak, D. M. Small, and G. G. Shipley, *Biochemistry* **15**, 4575 (1976).

- [27] T. P. W. McMullen, R. N. A. H. Lewis, and R. N. McElhaney, *Biochim. Biophys. Acta* **1416**, 119 (1999).
- [28] H. Takahashi, K. Sinoda, and I. Hatta, *Biochim. Biophys. Acta* **1289**, 209 (1996).
- [29] W.-J. Sun, S. Tristram-Nagle, R. M. Suter, and J. F. Nagle, *Proc. Natl. Acad. Sci. U.S.A.* **93**, 7008 (1996).
- [30] K. Sengupta, V. A. Raghunathan, and J. Katsaras, *Phys. Rev. E* **68**, 031710 (2003).
- [31] W. H. Press, S. A. Teukolsky, W. T. Vetterling, and B. P. Flannery, *Numerical Recipes* (Cambridge University Press, Cambridge, 1992).
- [32] R. P. Rand, V. A. Parsegian, J. A. C. Henry, L. J. Lis, and M. McAlister, *Can. J. Biochem.* **58**, 959 (1980).
- [33] W. Helfrich, *Z. Naturforsch. C* **28**, 693 (1973).
- [34] P. Méléard, C. Gerbeaud, T. Pott, L. Fernandez-Puente, I. Bivas, M. Mitov, J. Dufourcq, and P. Bothorel, *Biophys. J.* **72**, 2616 (1997).